Isospin effects on particle emission time sequence in $E/A=61$ MeV ^{36}Ar+^{112,124}Sn reactions

R. Ghetti,[1,*] J. Helgesson,[2] V. Avdeichikov,[3] B. Jakobsson,[1] N. Colonna,[4] and H. W. Wilschut[5]
[1]*Department of Physics, Lund University, Box 118, S-22100 Lund, Sweden*
[2]*School of Technology and Society, Malmö University, S-205 06 Malmö, Sweden*
[3]*Joint Institute for Nuclear Research, 141980 Dubna, Russia*
[4]*INFN and Dipartimento di Fisica, Via Amendola 173, I-70126 Bari, Italy*
[5]*Kernfysisch Versneller Instituut, Zernikelaan 25, NL-9747 AA Groningen, The Netherlands*
(Received 29 April 2004; published 3 September 2004)

The emission time sequence of neutrons, protons, and deuterons is deduced from velocity-gated two-particle correlation functions in $E/A=61$ MeV ^{36}Ar+^{112,124}Sn reactions. A dependence of the emission sequence on the isospin of the emitting source is observed.

DOI: 10.1103/PhysRevC.70.034601 PACS number(s): 25.70.Pq, 21.65.+f

The isospin dependence of the nuclear equation of state (EOS) is an essential property for the understanding of extremely asymmetric nuclei and nuclear matter, as it may occur in, e.g., nucleosynthesis in presupernova evolution of massive stars, supernova explosions, and neutron stars. Unfortunately, our current knowledge of the nuclear symmetry energy is still very poor [1]. An opportunity to study the isospin-dependence of the EOS is provided by heavy ion collisions with isotope separated beam and/or target nuclei, where excited systems are created with different degree of neutron/proton ratio. Several observables have been predicted to be isospin dependent, e.g., the preequilibrium neutron/proton ratio [2], isospin fractionation [3–6], isoscaling in multifragmentation [7], neutron and proton flows [8], and, recently, the two-nucleon correlation function [9,10].

Two-particle correlation functions, measured in E/A = MeV ^{36}Ar-induced collisions on isotope-separated targets of ^{112}Sn and ^{124}Sn, have been presented in Ref. [11]. Both angle-integrated and total-momentum gated correlation functions of particle pairs including neutrons, protons, deuterons, and tritons were measured and sizable isospin effects were observed particularly in *np*, and also in *pp*, *pt*, *nd*, and *nt*. In this paper we extend the data analysis of Ref. [11] to investigate the sequence of emission of neutrons, protons, and deuterons.[1] A preliminary report was presented in Ref. [12]. This analysis shows that an isospin signature can be derived also from the particle emission sequence.

The experiment was performed at the AGOR Superconducting Cyclotron of KVI (Groningen), with an interferometer consisting of 16 CsI(Tl) detectors for light charged particles [13] and 32 liquid scintillator neutron detectors [14]. 32 phoswich modules from the KVI Forward Wall were utilized as low-bias time marker to resolve the ambiguities caused by the time structure of AGOR [14]. In this work, particles detected in the angular range $30° \leqslant \theta \leqslant 120°$ are utilized, with energy thresholds of 2, 8, and 11 MeV for *n*, *p*, and *d*, respectively. Details about the experimental arrangements can be found in Refs. [11,13–15].

The correlation function,

$$C(\mathbf{q},\mathbf{P}_{tot}) = k\frac{N_c(\mathbf{q},\mathbf{P}_{tot})}{N_{nc}(\mathbf{q},\mathbf{P}_{tot})}, \quad (1)$$

is constructed by dividing the coincidence yield (N_c) by the yield of noncorrelated events (N_{nc}) generated from the product of the singles distributions [16]. $\mathbf{q}=\mu(\mathbf{p}_1/m_1-\mathbf{p}_2/m_2)$ is the relative momentum, μ is the reduced mass, $\mathbf{P}_{tot}=\mathbf{p}_1+\mathbf{p}_2$ is the total momentum of the particle pair, and k is a constant to normalize the correlation function to unity at large values of q ($80<q<120$ MeV/c for *np*, $120<q<150$ MeV/c for *nd*, and $150<q<200$ MeV/c for *pd*).

The strength of the correlation function depends on the space-time extent of the particle emitting source. For $E/A \sim 60$ MeV midperipheral reactions, the situation is complicated by the fact that emission of light particles originates from (at least) three sources; a projectilelike source (PLS), a targetlike source (TLS), and an intermediate velocity source (IS). The IS is responsible for dynamical emission (DE), which is described by early nucleon-nucleon collisions and by other preequilibrium processes, such as neck emission for noncentral collisions. Indeed, the source analysis of Ref. [17], based on the single-particle invariant energy spectra, has demonstrated that $E/A=61$ MeV ^{36}Ar+^{112,124}Sn data comprise particles emitted from the TLS and from the IS. Detection of particles emitted from the PLS is instead suppressed, due to the lack of forward angle coverage of our apparatus.

A classical way to bias the data sample toward emission from the different sources is by introducing cuts in the total momentum of the particle pair, calculated in the emitting source frame [16]. The distributions of total momentum for the $E/A=61$ MeV ^{36}Ar+^{124}Sn reaction are presented in Fig. 1, for the different particle pairs. For each type of particle pair, the P_{tot} distributions are calculated in two different source frames, a TLS frame (source velocity $\sim 0.02c$, left panels), and an IS frame (source velocity $\sim 0.18c$, right panels). These source velocities are defined in [17]. In line with

*Corresponding author; Email address: roberta.ghetti@nuclear.lu.se

[1]Results from the analysis of *pt*, *dt*, and *nt* correlation functions will appear in a forthcoming paper.

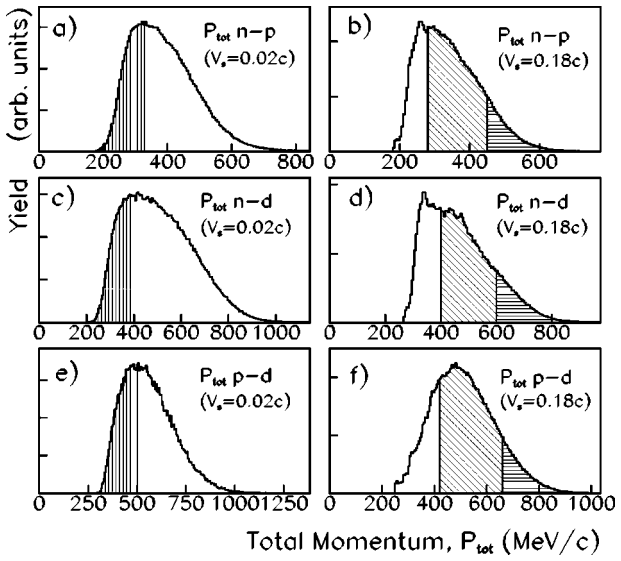

FIG. 1. For the $E/A=61$ MeV ^{36}Ar+^{124}Sn reaction, distributions of total momentum of the particle pairs calculated in the TLS frame ($v_s \sim 0.02c$), left panels, and in the IS frame ($v_s \sim 0.18c$), right panels, for *np* pairs [panels (a,b)], *nd* pairs [panels (c,d)], and *pd* pairs [panels (e,f)]. The hatched areas represent the total momentum gates applied in the analysis.

the procedure presented in Ref. [11], the following three total momentum gates are applied in the data analysis:

i) Particles emitted by the IS at prompt DE stage, such as first-chance nucleon-nucleon collisions, are enhanced by selecting high-P_{tot} pairs in the IS frame [horizontally hatched areas in Figs. 1(b,d,f)].

ii) Particles emitted by the IS at later DE stage, such as neck emission, are enhanced by selecting intermediate-P_{tot} pairs in the IS frame [diagonally hatched areas in Figs. 1(b,d,f)].

iii) Particles emitted by the TLS are enhanced by selecting low-P_{tot} pairs in the TLS frame [vertically hatched areas in Figs. 1(a,c,e)]. To further surpress the contribution from the IS source we only use detectors in the angular range $54° \leqslant \theta \leqslant 120°$, and we use the energy threshold of 8 MeV for neutrons, (see [11]).

It should be noticed that the choice of the total momentum gates for this analysis is determined empirically, by taking the minimum width allowed by the constraints imposed by the statistics of the particle-velocity gated correlation functions, and by the range of relative momentum needed for normalization of the correlation functions. However, in many cases, we might have chosen a larger width without affecting the results. The sensitivity to the gating conditions is further discussed Ref. [11]. The use of total momentum gates does not guarantee that the selection of the kinematic sources is exclusive. Contributions from other sources are not excluded, and there is some overlap of the event classes contributing to the kinematic regions defined by the different total momentum cuts [11].

In the correlation function analysis of Ref. [11], sizable isospin effects were revealed at a total momentum selection corresponding to gate ii). More pronounced *pp* and *np* correlation functions were observed for the neutron-rich ^{36}Ar +^{124}Sn system, as compared to ^{36}Ar+^{112}Sn. Since from the size of the source a stronger correlation is expected for the smaller ^{36}Ar+^{112}Sn system, the more pronounced correlation observed in the ^{36}Ar+^{124}Sn system was interpreted as an isospin effect, connected with a faster time scale for particles emitted at the later stages of the DE [11]. This could, for example, be explained by the density dependence of the nuclear symmetry energy in the neck region. Neutrons are expected to be emitted faster in the neutron-rich system, which would lead to an enhancement of the correlation strength for ^{36}Ar+^{124}Sn.

The time sequence of emission of the different light particles is deduced from the particle-velocity gated correlation functions, in a model independent way [18,19]. For nonidentical particle pairs, say *a* and *b*, we construct the correlation functions $C_a(q)$, gated on pairs with $v_a > v_b$, and $C_b(q)$, gated on pairs with $v_b > v_a$. If particle *a* is emitted later (earlier) than particle *b*, the ratio C_a/C_b must show a peak (dip) in the region of q where there is a correlation, and a dip (peak) in the region of q where there is an anticorrelation. The particle velocities are calculated in the frame of the emitting source.

Before discussing the experimental results for the emission time sequence, we remark that this kind of analysis yields information on the *average* emission time. To interpret the results correctly, one should be aware that a different average emission time can have various origins. The most obvious mechanism is a simple time shift of the time distributions of the two particles. However, a different average emission time can occur even if there is no time shift between the two distributions. For instance, the width of the two time distributions could be different. A third possibility is when more than one source is contributing. If the yield of the two particle types is different for one of the sources, the average emission times will be different, even if the width and shift of the time distributions are equal. Probably all these mechanisms contribute, but to a different degree, depending on particle types, applied gates, detection angles, etc.

The particle-velocity gated analysis of the *np* correlation function is presented in Fig. 2 for ^{36}Ar+^{112}Sn (left column) and ^{36}Ar+^{124}Sn right column). For each P_{tot}-gate, we present $C_n(q)$, gated on pairs $v_n > v_p$ (black dots), $C_p(q)$, gated on pairs $v_p > v_n$ (open circles), and their ratio, $C_n(q)/C_p(q)$ (star symbols). The results for the *n*-*p* emission time sequence are the following.

i) For the high-P_{tot} gate [Figs. 2(a,c)], the strength of the correlation function comes mainly from pairs with $v_p > v_n$, contributing to C_p (open circles). The ratio C_n/C_p has a pronounced dip at low relative momenta [Figs. 2(b,d)], indicating that, for these high-P_{tot} pairs, neutrons are, on average, emitted earlier than protons. This result, very similar for the two Sn targets, may indicate that neutron emission is favored in first chance nucleon-nucleon collisions, because of the N/Z ratio of the systems under study.

ii) For the intermediate region of P_{tot} [Figs. 2(e,g)], the dip in the C_n/C_p ratio becomes less pronounced, indicating that the average emission times of neutron and protons are more similar to each other. Furthermore, comparing Figs. 2(e,g), one can see that: 1) The strength of the (total) correlation function is slightly larger for the neutron-rich system,

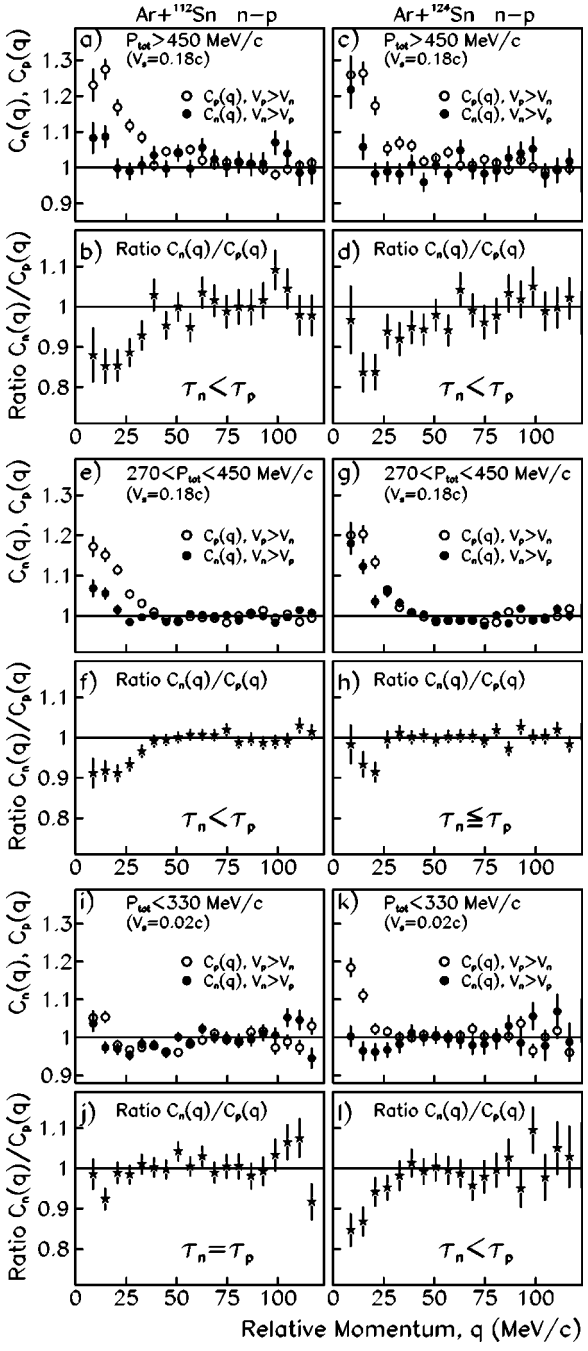

FIG. 2. Neutron-proton velocity-gated correlation functions and their ratio deduced from $E/A=61$ MeV ^{36}Ar+^{112}Sn (left column) and ^{36}Ar+^{124}Sn (right column) reactions.

^{36}Ar+^{124}Sn. 2) The C_p and C_n correlation functions are more similar to each other for ^{36}Ar+^{124}Sn than for ^{36}Ar+^{112}Sn. Since these isospin signals appear to be associated with the particles selected by the intermediate-P_{tot} gate, and to be washed out by the high-P_{tot} gate, they may be connected with the density dependence of the nuclear symmetry energy [9,10]. The calculations in Ref. [9] indicate that a stiff symmetry potential causes high momentum neutrons and protons to be emitted faster (and almost simultaneously) as compared to a soft parametrization, that delays proton emission. In particular, the average emission times of protons (τ_p) and neutrons (τ_n) calculated as a function of their momenta with the stiff potential, display a "switch" in the emission time sequence for neutrons and protons, going from $\tau_n < \tau_p$ at high momenta [as in our results for gate i), Figs. 2(b,d)] to $\tau_n \approx \tau_p$ at intermediate momenta [as in our results for the ^{124}Sn target in gate ii), Fig. 2(h)]. Of course more appropriate calculations need to be performed for our specific systems before definite conclusions on the symmetry potential can be drawn.

iii) Finally, as one selects low-P_{tot} pairs in the TLS frame [Figs. 2(i,k)], thus enhancing TLS emission, the result is that the overall strength of the correlation function decreases as compared to the ungated correlation function. This is as expected, indicating that the TLS source, with long emission times, is enhanced. For the Ar+^{112}Sn system the two velocity gated correlation functions are quite similar to each other, with the C_n/C_p ratio close to unity [Fig. 2(j)]. Since the time distribution from an evaporative source is expected to be wider for neutrons than protons (because of the Coulomb barrier for protons), one would expect to find the C_n/C_p ratio larger than unity, indicating a larger average emission time for neutrons than for protons. Notice that the chronology analysis performed on data from $E/A=61$ MeV ^{36}Ar+^{27}Al [15] and from $E/A=45$ MeV ^{58}Ni+^{27}Al [19] collisions yielded such a time sequence for neutrons and protons emitted from the PLS. The reason for not seeing a larger average neutron emission time in the Ar+^{112}Sn system might be that the contribution from the intermediate velocity source slightly shifts the average time (the selected P_{tot} gate surpresses the IS source, but it does not eliminate it). For the Ar+^{124}Sn system the situation is quite different. The strength of the correlation function mainly comes from pairs with $v_p > v_n$, and the dip in the C_n/C_p ratio [Fig. 2(l)] indicates that neutrons are, on average, emitted earlier than protons. The present result may be understood if one considers that the target residue formed in the collisions is neutron-rich, and therefore neutrons will evaporate first. Because the evaporated protons have a Coulomb barrier to penetrate, it is likely that neutrons will also be the last particles to be emitted from the TLS source [15]. However, the fact that for a neutron-rich system there are more neutrons evaporated at the beginning of the TLS deexcitation, gives an average emission time shorter for neutrons. Notice also that the strength of the correlation functions is larger for the ^{36}Ar+^{124}Sn system [cf. Figs. 2(i,k)]. This may indicate that the more asymmetric system generates a more asymmetric and excited TLS that, consequently, decays on a faster time scale [11].

We now turn to the results involving deuterons. Within the multisource reaction mechanism, composite particles, such as deuterons and tritons, are believed to be predominantly emitted from the DE source [20,21], where they are formed by a coalescence mechanism [17,22]. Nevertheless, a sensitivity to the isospin may be expected for correlation functions such as *nd* and *pd*, as a consequence of the isospin effects on neutrons and protons. The analysis of Ref. [11] has revealed small isospin effects in the *nd* correlation function and negligible isospin effects in *pd*.

The particle-velocity gated analysis of the *nd* correlation function is presented in Fig. 3 for ^{36}Ar+^{112}Sn (left column)

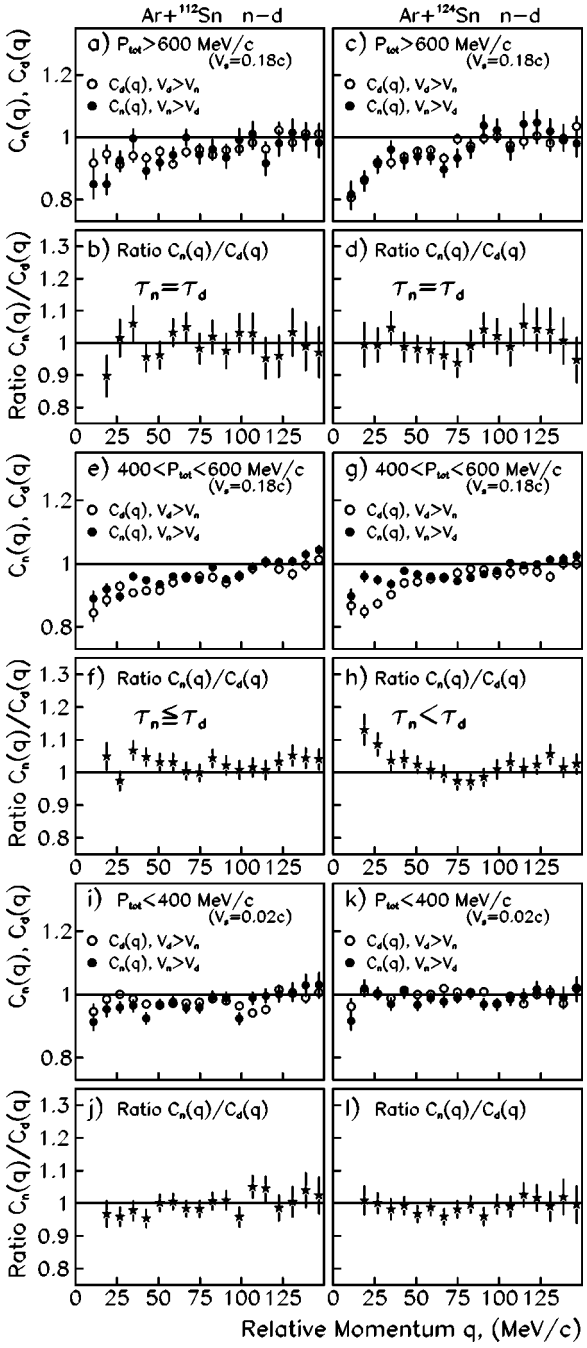

FIG. 3. Neutron-deuteron velocity-gated correlation functions and their ratio deduced from $E/A=61$ MeV ^{36}Ar+^{112}Sn (left column) and ^{36}Ar+^{124}Sn (right column) reactions.

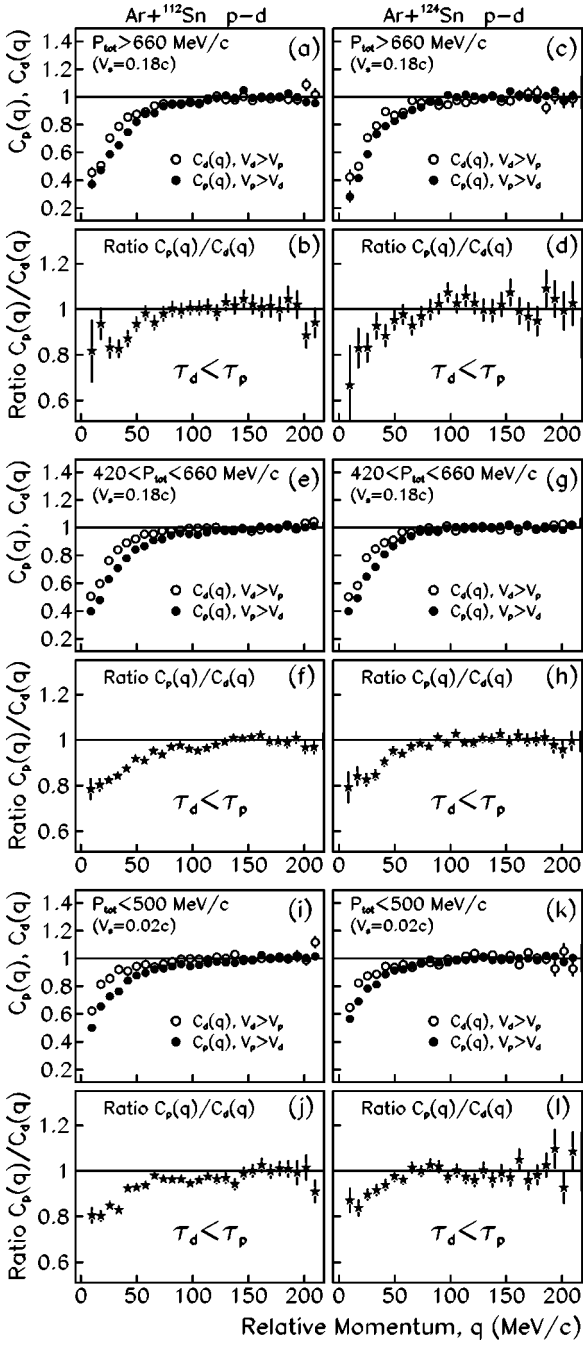

FIG. 4. Proton-deuteron velocity-gated correlation functions and their ratio deduced from $E/A=61$ MeV ^{36}Ar+^{112}Sn (left column) and ^{36}Ar+^{124}Sn (right column) reactions.

and ^{36}Ar+^{124}Sn (right column). Notations are the same as in Fig. 2. The general shape of the *nd* correlation function is a weak anticorrelation at low relative momentum. This shape, already observed at lower energies [23] and for a different system at 61 A MeV [15], may originate from the depletion of low relative momentum *nd* pairs due to triton formation [24].

We now proceed to discuss the results for the emission time sequence in the three applied P_{tot} gates.

i) Gating on the high momentum tail of the P_{tot} distribution, calculated in the IS reference frame, the strength of the *nd* anticorrelation becomes slightly stronger for ^{36}Ar+^{124}Sn [Fig. 3(c)], as compared to ^{36}Ar+^{112}Sn [Fig. 3(a)]. The two particle-velocity gated correlation functions, C_n and C_d, behave quite similarly to each-other, and the ratio $C_n(q)/C_d(q)$ tends to approach unity at all values of relative momentum, q [Figs. 3(b,d)], indicating that the average emission time of neutrons and deuterons is similar. Thus, it appears as if deuteron formation sets in rather early in the DE phase.

ii) Lowering the P_{tot} gate [Figs. 3(e,g)], in an attempt to select *nd* pairs from the later phases of DE and from neck emission, brings us into a regime where the average emission

sequence is that neutrons are emitted slightly earlier than deuterons. This is particularly true for the ^{36}Ar+^{124}Sn system [Fig. 3(h)], as may be expected since neutrons are emitted on a faster time scale in the more neutron-rich system [see the above discussion of Figs. 2(g,h)]. This result is consistent with deuterons being formed mainly by coalescence, with an average emission time that falls in-between that of neutrons and protons [15].

iii) Finally, as one selects low-P_{tot} pairs in the TLS frame [Figs. 3(i,k)], the *nd* correlation function becomes rather featureless. If *d* are formed in the DE stages of the collision, they should not correlate very much with particles evaporated at the later stages of statistical emission. This is indeed the case, as seen in Figs. 3(i,k).

The particle-velocity gated analysis for the *pd* correlation function is presented in Fig. 4 for ^{36}Ar+^{112}Sn (left column) and ^{36}Ar+^{124}Sn (right column). Notations are the same as in Fig. 2. The *pd* correlation function is characterized by a pronounced anticorrelation at small *q*, due to final state Coulomb repulsion. The anticorrelation is more pronounced for DE particle pairs selected by high- and intermediate-P_{tot} gates [Figs. 4(a,c,e,g)]. Nevertheless, an anticorrelation is found also for *pd* pairs selected by the TLS-gate [Figs. 4(i,k)] as may be expected because of the long range of the Coulomb force.

Comparing the results for ^{36}Ar+^{112}Sn (Fig. 4, left column) and for ^{36}Ar+^{124}Sn (Fig. 4, right column), one can see that, as already found in Ref. [11] for the integrated correlation functions, the isospin effects in the *pd* correlation functions are negligible.

Concerning the emission time sequence, we find that deuterons are, on average, emitted earlier than protons, for both Sn targets. Note that this result regards the average emission time, and that it does not exclude that prompt protons are emitted before any deuteron is emitted. The size of this effect is comparable for all studied P_{tot} gates, as indicated by the dip in the $C_p(q)/C_d(q)$ ratio, that reaches the value of ≈ 0.8 in all cases [Figs. 4(b,d,f,h,j,l)]. This emission time sequence for protons and deuterons is consistent with the findings of previous experimental investigations [15,25].

In summary, the emission time sequence of neutrons, protons, and deuterons has been investigated in the $E/A = 61$ MeV ^{36}Ar+^{112}Sn, ^{124}Sn reactions by analyzing velocity-gated correlation functions of nonidentical particle pairs. The extracted emission time sequences are the following:

i) High-P_{tot} gate: $\tau_n \approx \tau_d < \tau_p$,

ii) Intermediate-P_{tot} gate: $\tau_n \leqslant \tau_d < \tau_p$,

iii) Low-P_{tot} gate: τ_n, $\tau_d < \tau_p$.

Isospin effects are seen in the emission time sequence both in later DE (for *np* and *nd* correlation functions) and in TLS emission (for *np*). The isospin effects seen when a total momentum gate that enhances later DE (and possibly neck emission) is applied may reflect a dependence on the nuclear symmetry energy. Comparison of the present data set with theoretical calculations will impose strong constraints on the model description of the nuclear EOS.

This work was partly supported by the European Commission (Transnational Access Program, Contract No. HPRI-CT-1999-00109) and by the Swedish Research Council (Contract Nos. F 620-149-2001 and 621-2002-4609).

[1] *Isospin Physics in Heavy-Ion Collisions at Intermediate Energies*, edited by B.-A. Li and W. U. Schröder (Nova Science, New York, 2001).
[2] B.-A. Li *et al.*, Phys. Rev. Lett. **78**, 1644 (1997).
[3] V. Baran *et al.*, Nucl. Phys. **A703**, 603 (2002).
[4] B.-A. Li and C. M. Ko, Nucl. Phys. **A618**, 498 (1997).
[5] H. S. Xu *et al.*, Phys. Rev. Lett. **85**, 716 (2000).
[6] W. P. Tan *et al.*, Phys. Rev. C **64**, 051901(R) (2001).
[7] M. B. Tsang *et al.*, Phys. Rev. Lett. **86**, 5023 (2001).
[8] B.-A. Li *et al.*, Phys. Rev. C **64**, 054604 (2001).
[9] L. W. Chen *et al.*, Phys. Rev. Lett. **90**, 162701 (2003).
[10] L. W. Chen *et al.*, Phys. Rev. C **68**, 014605 (2003).
[11] R. Ghetti *et al.*, Phys. Rev. C **69**, 031605(R) (2004).
[12] R. Ghetti *et al.*, Nucl. Phys. **A734c**, 597 (2004).
[13] V. Avdeichikov *et al.*, Nucl. Instrum. Methods Phys. Res. A **501**, 505 (2003).
[14] R. Ghetti *et al.*, Nucl. Instrum. Methods Phys. Res. A **516**, 492 (2004).
[15] R. Ghetti *et al.*, Phys. Rev. Lett. **91**, 092701 (2003).
[16] R. Ghetti *et al.*, Nucl. Phys. **A674**, 277 (2000).
[17] V. Avdeichikov *et al.*, Nucl. Phys. **A736**, 22 (2004).
[18] R. Lednicky *et al.*, Phys. Lett. B **373**, 30 (1996).
[19] R. Ghetti *et al.*, Phys. Rev. Lett. **87**, 102701-1 (2001).
[20] G. Lanzanò *et al.*, Nucl. Phys. **A683**, 566 (2001).
[21] T. Lefort *et al.*, Nucl. Phys. **A662**, 397 (2000).
[22] W. J. Llope *et al.*, Phys. Rev. C **52**, 2004 (1995).
[23] R. A. Kryger *et al.*, Phys. Rev. Lett. **65**, 2118 (1990).
[24] L. Tomio *et al.*, Phys. Rev. C **35**, 441 (1987).
[25] D. Gourio *et al.*, Eur. Phys. J. A **7**, 245 (2000).